Microwave-assisted synthesis, molecular docking and anti-HIV activities of some drug-like quinolone derivatives

Ahmed M. Jassem, Adil M. Dhumad, Faeza A. Almashal & Jasim M. Alshawi

Medicinal Chemistry Research

ISSN 1054-2523
Volume 29
Number 6

Med Chem Res (2020) 29:1067-1076
DOI 10.1007/s00044-020-02546-z

Springer

Medicinal Chemistry Research (2020) 29:1067–1076
https://doi.org/10.1007/s00044-020-02546-z

MEDICINAL CHEMISTRY RESEARCH

ORIGINAL RESEARCH

Microwave-assisted synthesis, molecular docking and anti-HIV activities of some drug-like quinolone derivatives

Ahmed M. Jassem[1] · Adil M. Dhumad[1] · Faeza A. Almashal[1] · Jasim M. Alshawi[1]

Received: 18 February 2020 / Accepted: 10 April 2020 / Published online: 29 April 2020

Abstract

In targeted therapy of breast cancer, human epidermal growth factor receptor 2 HER2 (PDB ID: 3PP0) is being considered as a promising route to design novel anti-breast cancer drugs. In this work, we report two of novel *N*-substituted pyrrolidine at C-8 position of quinolone derivatives **18** and **19**, their synthesis under microwave technique, spectral methods, molecular docking study and anti-HIV activities. Docking study exhibited hydrogen bonding, polar, and Van der Waals interactions with the active site residues of HER2 target. The binding energy and hydrogen bonding interactions show that synthesized compounds are being considered to have a potential activity against breast cancer. In addition, quinolone derivatives were evaluated in vitro for antiviral activity against the replication of HIV-1 and HIV-2 in MT-4 cells. The results showed that quinolone derivatives **18** and **19** possess a potent activity against HIV-1 replication with IC_{50} values of ≥15.20 and 14.26 μM, SI ≤ 6 and >7, respectively.

Keywords Microwave synthesis · Breast cancer · HER2 (PDB ID: 3PP0) · Molecular docking · Anti-HIV activities · Quinolone derivatives

Introduction

Cancer is an incurable disease, originating from uncontrolled proliferation of cells with the potential to permeate to other organs of body (Sravanthi et al. 2019). Breast cancer is a malignant and deadly disease in the world because the current treatments are limited by the emergence of the cure-resistant cancer cells (Siegel et al. 2011; Stockler et al. 2000). Human epidermal growth factor receptor 2 HER2 (PDB ID: 3PP0) is a protooncogene, which has an important role in the regulation of cyclic cell signaling pathways involving cell proliferation and cellular replication. HER2 appears to be involved in 20% of diagnosed breast cancer. A considerable evidence indicates that HER2 (PDB ID: 3PP0) protein is expected to mutate in HER2-positive breast cancer, that leads to defective control of malignant transformation and cellular proliferation (Dent et al. 2013; Pinhel et al. 2012). Thus, targeting HER2 may be considered as a potential target for breast cancer therapy.

Quinolones are one of a common moiety in antibiotic structures such as enoxacin **1** (Vracar et al. 2018), ciprofloxacin **2** (Mitscher 2005), lomefloxacin **3** (Beberok et al. 2017), fleroxacin **4** (Zelmat et al. 2020), ofloxacin **5** (Dubar et al. 2011) and nalidixic acid **6** (Appelbaum and Hunter 2000; Bisacchi 2015; Jacoby 2005) (Fig. 1). These drugs are widely used as an effective treatment against bacterial infections, including an infectious respiratory, pneumonia, diarrhea, gonorrhea, typhoid fever and urinary tract infections (Dalhoff 2015; Naqvi et al. 2018). Due to a high intracellular penetration and good oral bioavailability of some quinolone derivatives (Anquetin et al. 2005; Baker et al. 2004), they play a vital role as an efflux pump inhibitor (Chevalier et al. 2001), antimicrobial activity (Jardosh and Patel 2013), apicoplastic (Dahl and Rosenthal 2007), anti-tuberculosis (Wohlkonig et al. 2010) and anti-leprosy (moxifloxacin **7**) (Laponogov et al. 2009; Wohlkonig et al. 2010). The compound **7** can form a reversible ternary complex via binding with two type of bacterial targets (topoisomerase IV enzymes and DNA gyrase) that leads to block the bacterial growth (Drlica et al. 2009; Drlica and

Supplementary information The online version of this article (https://doi.org/10.1007/s00044-020-02546-z) contains supplementary material, which is available to authorized users.

✉ Ahmed M. Jassem
ahmed.majedd@uobasrah.edu.iq

[1] Department of Chemistry, College of Education for Pure Sciences, University of Basrah, Basrah, Iraq

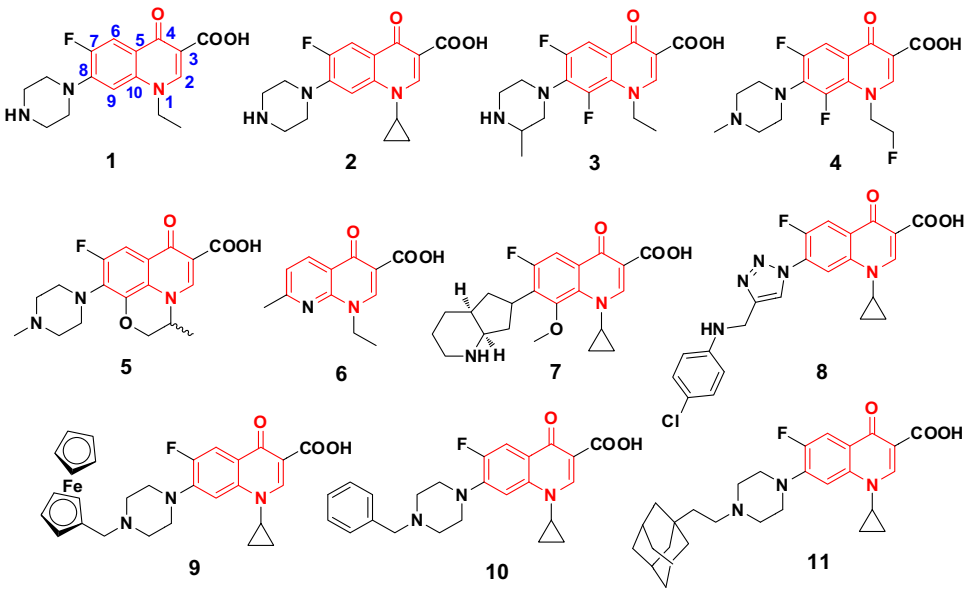

Fig. 1 Chemical structures of some pharmacological-quinolone derivatives

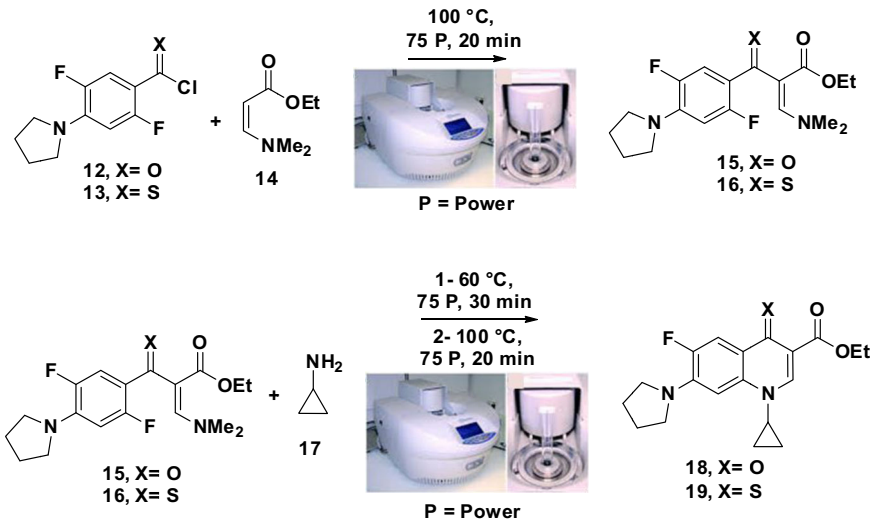

Scheme 1 Microwave synthesis of quinolone derivatives **18** and **19**

Malik 2003). On the other hand, quinolone derivatives have offered significant anti-HIV activities. Examples of anti-HIV activities of quinolone derivatives include HIV-1 protease inhibition such as 6-aminoquinolone derivatives and quinolone-3-carboxylic acid derivatives (Hajimahdi et al. 2016).

The C-8 position is an essential place for enhancing pharmacological activities as emerged by the crystal structure from the interaction between moxifloxacin **7** and topoisomerase IV (Wohlkonig et al. 2010). Therefore, the modifications at the C-8 position have been investigated in order to explore the advantages of the interaction between C-8 position and binding site (pocket of DNA gyrase) (Matrat et al. 2007, 2008). Triazole substituted at C-8 position of compound **8** enhanced the pharmacological effect of compound **8** against microbial (Patpi et al. 2012; Shanmugavelan et al. 2011; Sumangala et al. 2010). The replacement of a ferrocenic piperazine core (compound **9**) instead of triazole group showed an additional enhancement of anti-plasmodial activity (Dubar et al. 2008) due to the redox properties and high lipophilicity of a ferrocenic group (Chavain et al. 2008). Grafting a phenyl group (compound **10**) or an adamantanyl moiety (compound **11**) instead of the ferrocenic group at C-8 position prevents the ability to catalyze a Fenton-like reaction which results during the production of hydroxyl radicals. Although Bayer et al. reported and patented a seven-step synthesis of ciprofloxacin **2** in the 1980s with an overall yield of 49%, the efficient methods for the synthesis of quinolone derivatives are highly needed (Payne et al. 2006; Spellberg et al. 2015).

Microwave technique is known and emerged as an efficient methodology in modern organic synthesis (Kappe and Dallinger 2009). Microwave irradiation (MW) technique mostly enhances reaction rates, increases product yields

(Shaabani and Bazgir 2004), reduces the reaction times (Maiti and Chanda 2016), enables precise control of the reaction conditions, promotes solvent-free reactions (Amore et al. 2006; Jida et al. 2010; Seijas et al. 2008), eco-friendly approach, and improved regioselectively (Driowya et al. 2016; Kumar et al. 2015; Kumar et al. 2018). In continuation of our work to utilize the advantages of microwave irradiation, we aim to use microwave technique for the synthesis of quinolone derivatives as shown in Scheme 1. Moreover, as a part of our search into the view of varied pharmacological activities of quinolone derivatives, we report the molecular docking calculations of the synthesized quinolone derivatives **18** and **19** in order to identify their binding interactions with the target protein HER2 (PDB ID: 3PP0). Finally, the cytotoxicity of these derivatives on anti-HIV activities has been evaluated.

Material and methods

Chemistry

All chemicals were ordered from Sigma-Aldrich (Saint Louis, USA). All microwave reactions were carried out by using Smith Creator™ Optimiser EXP reactor (Vials™). TLC experiments were done by using plates precoated with silica gel 60. The plates were visualized under UV 254 and an aqueous potassium permanganate. Final purification of the synthesized compounds was performed using column chromatography with silica gel 60 Å (230–400 mesh). Melting points were measured in open capillary tubes on a Gallenkamp melting point apparatus. Fourier transform infrared (FT-IR) analysis was recorded by using on a Perkin Elmer Paragon 100 FT-IR spectrophotometer in the range of 4000–750 cm^{-1}. Nuclear magnetic resonance (^{1}H, ^{9}F and ^{13}C NMR) spectra were recorded on Bruker AV-400 (400 Hz) and on Bruker AV-400 (100.5 Hz) spectrometer in deuterated dimethyl sulfoxide as solvent (^{1}H NMR: DMSO-d_6: δ 2.50 ppm; ^{13}C NMR: DMSO-d_6: δ 39.52 ppm). The δ values are given in ppm and the coupling constants J are evaluated by Hz unite. Micro Mass LCT operating in Electrospray mode (ES) was used to determine the molecular weights of the synthesized compounds. HPLC analysis for the synthesized compounds were carried out by using Waters Xbridgea C18 5µm column (4.6 mm × 255 mm); 5 − 95% acetonitrile/aqueous TFA (0.1%) over 20 min, hold 10 min; UV detection at 254 nm.

General microwave synthesis of compounds (15 and 16)

All microwave reactions were carried out in a capped (10 mL) microwave-vessel (Borosilicate glass vial sealed) that was placed in a microwave cavity. The pressure was set at 17 bar (average of an effective pressure = 4 bar) with power 75 W. DIEA (3.4 g, 3.4 mmol) was added to a solution of either 2,5-difluoro-4-(pyrrolidin-1-yl) benzoyl chloride **12** (0.83 g, 3.4 mmol) or 2,5-difluoro-4-(pyrrolidin-1-yl)benzothioyl chloride **13** (0.88 g, 3.4 mmol) and ethyl-3-(diethylamino)acrylate **14** (0.45 g, 3.1 mmol) in acetonitrile (5 mL). The mixture reaction was held at 100 °C for 20 min. After the reaction vessel was cooled to room temperature, the crude product was diluted with water (10 mL) and extracted with ethyl acetate (3 × 10 mL). The organic layers were combined, dried over Na_2SO_4, filtered, evaporated and purified by a flash column chromatography (eluent *n*-hexane: acetone, 3:1) to give the titled compounds.

Ethyl-2-(2,5-difluoro-4-(pyrrolidin-1-yl)benzoyl)-3-(dimethylamino) acrylate (15)

Yellow oil ($R_f = 0.3$), Yield 85%. IR (KBr) ν_{max} in cm^{-1}: 2993 (C–H, Ar), 2953 (C–H), 1760 (C=O), 1692 (C=O), 1654 (C=C, Ar), 1592 (C–N). ^{1}H NMR (400 MHz, DMSO-d_6): $\delta = 7.77$ (1H, s, CH), 7.32 (1H, d, $J = 5.0$ Hz, CH–Ar), 6.88 (1H, d, $J = 5.2$ Hz, CH–Ar), 4.2 (2H, q, $J = 7.1$ Hz, CH_2), 3.47-3.42 (4H, m, $2CH_2$), 3.1 (6H, s, $2CH_3$), 2.01-1.97 (4H, m, $2CH_2$), 1.32 (3H, t, $J = 4.2$ Hz, CH_3).

Ethyl-2-(2,5-difluoro-4-(pyrrolidin-1-yl) phenylcarbonothioyl)-3-(dimethylamino) acrylate (16)

Orange oil ($R_f = 0.4$), Yield 80%. IR (KBr) ν_{max} in cm^{-1}: 2982 (C–H, Ar), 2894 (C–H), 2868 (C–H), 1718 (C=O), 1595 (C=C, Ar), 1581 (C–N), 1023 (C=S). ^{1}H NMR (400 MHz, DMSO-d_6): $\delta = 7.41$ (1H, s, CH), 6.72 (1H, d, $J = 4.0$ Hz, CH–Ar), 6.68 (1H, d, $J = 3.6$ Hz, CH–Ar), 4.19 (2H, q, $J = 4.3$ Hz, CH_2), 3.42-3.40 (4H, m, $2CH_2$), 3.04 (6H, s, $2CH_3$), 1.95-1.92 (4H, m, $2CH_2$), 1.29 (3H, t, $J =$ 5.4 Hz, CH_3).

General microwave synthesis of quinolone derivatives (18 and 19)

To a solution of compound **15** (0.26 g, 0.75 mmol) or compound **16** (0.26 g, 0.72 mmol) in a mixture of ethanol/diethyl ether (1:2, 5 mL), cyclopropylamine **17** (0.1 mL, 1.4 mmol) was added. After 10 min of stirring at 60 °C under microwave (an effective pressure = 4 bar and power 75 W), the resulting mixture was cooled to room temperature and evaporated under vacuum to give an orange oil. To a solution of orange oily residue dissolved in DMSO (5 mL), 1,8-diazabicyclo [5.4.0]undec-7-ene (DBU) (0.39 g, 2.56 mmol) was added and stirred

under microwave at 150 °C for 25 min. The resulting mixture was diluted with cold water (5 mL) and washed with an aqueous solution of NH_4Cl (5 mL). The combined organic layers were additionally washed with water three times, dried over Na_2SO_4, filtered and concentrated. The orange precipitate residue was purified by a flash column chromatography (eluent dichloromethane: methanol, 12:1). The fractions that contain compounds **18** and **19** were dried and thoroughly washed with diethyl ether three times to give the titled quinolone derivatives.

Ethyl-1-cyclopropyl-6-fluoro-4-oxo-7-(pyrrolidin-1-yl)-1,4-dihydro quinolone-3-carboxylate (18)

Orange solid ($R_f = 0.4$), Yield 80%, mp 212-213 °C. IR (KBr) ν_{max} in cm^{-1}: 2981 (C–H, Ar), 2906 (C–H), 1720 (C=O), 1689 (C=O), 1619 (C=C, Ar), 1590 (C–N). ^1H NMR (400 MHz, DMSO-d_6): $\delta = 8.30$ (1H, s, H-2), 7.60 (1H, d, $J = 8.2$ Hz, H-6), 6.91 (1H, d, $J = 7.6$ Hz, H-9), 4.22-4.14 (2H, m, H-12), 3.54 (4H, t, $J = 4.4$ Hz, H-16, H-16"), 3.52-3.48 (1H, m, H-14), 1.98-1.94 (4H, m, H-17, H-17"), 1.25 (3H, t, $J = 7.0$ Hz, H-13), 1.24-1.04 (4H, m, H-15, H-15"). ^{19} F NMR (100 MHz, DMSO-d_6): $\delta = -129.9$ (F, C-7). ^{13}C NMR (100 MHz, DMSO-d_6): $\delta = 171.8$ (C=O, C-4), 165.7 (C=O, C-11), 150.5 (C, C-7, d, $J =$ 20 Hz), 148.5 (C, C-8, d, $J = 21$ Hz), 140.8 (CH, C-2), 139.7 (C, C-10), 118.0 (C, C-5), 111.6 (CH, C-6), 109.2 (C, C-3), 60.3 (CH_2, C-12), 50.4 (CH_2, C-16, C-16"), 43.9 (CH, C-14), 25.4 (CH_2, C-17, C-17"), 14.7 (CH_3, C-13). HRMS (ESI^+) *m/z*: 345.1609 for $C_{19}H_{21}FN_2O_3$ ($[M + H]^+$) (calcd. 345.1611).

Ethyl-1-cyclopropyl-6-fluoro-7-(pyrrolidin-1-yl)-4-thioxo-1,4-dihydro quinolone-3-carboxylate (19)

Red solid ($R_f = 0.4$), Yield 76%, mp 221-222 °C. IR (KBr) ν_{max} in cm^{-1}: 2981 (C–H, Ar), 2954 (C–H, Ar), 2870 (C–H), 1715 (C=O), 1575 (C=C), 1562 (C–N), 1038 (C=S). ^1H NMR (400 MHz, DMSO-d_6): $\delta = 8.34$ (1H, d, $J =$ 12.2 Hz, H-6), 8.10 (1H, s, H-2), 6.97 (1H, d, $J = 4.0$ Hz, H-9), 4.26-4.19 (2H, m, H-12), 3.70-3.63 (1H, m, H-14), 3.60-3.53 (4H, t, $J = 3.2$ Hz, H-16, H-16"), 2.0-1.93 (4H, m, H-17, H-17"), 1.28 (3H, t, $J = 7.1$ Hz, H-13), 1.26-1.10 (4H, m, m, H-15, H-15"). ^{19} F NMR (100 MHz, DMSO-d_6): $\delta = -127.6$ (F, C-7). ^{13}C NMR (100 MHz, DMSO-d_6): $\delta =$ 186.1 (C=S, C-4), 166.7 (C=O, C-11), 152.2 (C, C-7, d, $J = 24$ Hz), 150.3 (C, C-8, d, $J = 23$ Hz), 137.4 (CH, C-2), 126.1 (C, C-10), 115.0 (C, C-5), 114.7 (CH, C-6), 99.8 (C, C-3), 60.9 (CH_2, C-12), 50.3 (CH_2, C-16, C-16"), 39.5 (CH, C-14), 25.4 (CH_2, C-17, C-17"), 14.5 (CH_3, C-13). HRMS (ESI^+) *m/z*: 361.1381 for $C_{19}H_{21}FN_2O_2S$ ($[M + H]^+$) (calcd. 361.1382).

Theoretical calculations

The geometries of compounds **18** and **19** were fully optimized by using density functional theory (DFT) calculations with a 6–311G (d, p) basis set. The exchange-correlation potential has been evaluated by using hybrid functional B3LYP (Lee et al. 1988). After the optimization was completed, the frequencies calculations were performed to identify all the stationary points at the same computational level.

The molecular docking calculations of the synthesized compounds were performed by employing the software Auto-dock Vina (DS 2017 R2 Client) and the Auto-dock tools (DS 2017) graphical user interface was utilized to calculate the Gasteiger-Marsili charges. Polar hydrogen was added to identify the binding interactions with the target protein HER2 (PDB ID: 3PP0) (Trott and Olson 2010). The target protein was taken as a rigid body and the ligands are being to be flexible. The best binding model was chosen based on the lowest binding energy.

In vitro anti-HIV assay

In vitro anti-HIV assay, the evaluation of antiviral activity of the synthesized quinolone derivatives (**18** and **19**) against HIV-1 (strain III_B) and HIV-2 (strain ROD) in MT-4 cells was performed by using an MTT assay as described previously (Pauwels et al. 1988). The MT-4 cells were made by co-cultivating leukocytes from an adult T-cell leukemia (ATL) patient with cord blood leukocytes (CBL). In brief, stock solutions (10 times final concentration) of tested compounds in volumes (50-µL) were added to two series of triplicate wells in order to allow a simultaneous evaluation of their effects on mock and HIV-infected cells at the beginning of each experiment. Serial 5-fold dilutions of tested compounds were prepared directly in flat-bottomed 96-well microtiter trays by using a Biomek 3000 robot (Beckman instruments). Untreated control, HIV-infected, and mock-infected cell samples were included for each sample. HIV-1 (III_B) and HIV-2 (ROD) stock (50 µL) at 100–300 CCID 50 (50% cell culture infectious dose) or culture medium [10% Fetal Calf Serum (FCS, heat-inactivated and suitable for cell culture, Sigma-Aldrich), 2 mM-glutamine, 0.1% sodium bicarbonate, and 20 µg/mL gentamicin] were added to either of infected or mock-infected wells of the microtiter tray. The mock-infected cells were used to evaluate the effect of tested compounds on uninfected cells in order to evaluate the cytotoxicity of the tested compounds. Exponentially, growth of MT-4 cells were centrifuged for 5 min at 1000 rpm (Minifuge T, rotor 2250) and the supernatant was discarded. The MT-4 cells were re-suspended at 6×105 cells per mL. Thus, volumes (50 µL) were transferred to the microtiter tray wells. After

Table 1 The optimal conditions for the synthesis of intermediate 15

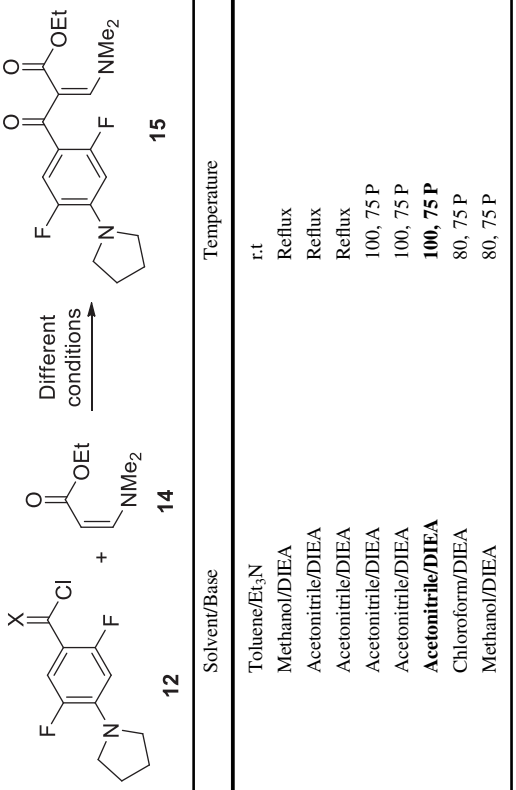

Entry	Method	Solvent/Base	Temperature	Time	Yield %[a]
1	Batch	Toluene/Et_3N	r.t	48 h	0
2	Batch	Methanol/DIEA	Reflux	24 h	20
3	Batch	Acetonitrile/DIEA	Reflux	24 h	30
4	Batch	Acetonitrile/DIEA	Reflux	48 h	35
5	MW	Acetonitrile/DIEA	100, 75 P	5 min	–
6	MW	Acetonitrile/DIEA	100, 75 P	10 min	34
7	**MW**	**Acetonitrile/DIEA**	**100, 75 P**	**20 min**	**85**
8	MW	Chloroform/DIEA	80, 75 P	20 min	52
9	MW	Methanol/DIEA	80, 75 P	20 min	35

[a]Isolated as a pure product

five days of an infection, the viability of the mock-infected and HIV-infected cells were determined by spectrophotometric method.

Results and discussion

Firstly, the synthesis of the intermediate **15** which requires an alkaline condition of a coupling reaction was investigated. The synthesis of the intermediate **15** started from the reaction between 2,5-difluoro-4-(pyrrolidin-1-yl) benzoyl chloride **12** and ethyl 3-(diethylamino)acrylate **14** to yield the intermediate **15**. Although under batch conditions in the presence of solvent/base: toluene/triethylamine (Et_3N) no yield was obtained (Table 1, entry 1), the desired product **15** was isolated in low yields in the presence of solvent/base: methanol/N,N-diisopropylethylamine (DIEA) and acetonitrile/DIEA (Table 1, entries 2–4). Therefore, switching over to microwave conditions afforded rise to improve the coupling reaction. To test the simplicity of a microwave reaction, the optimal conditions of the model reaction were carried out in the presence of three systems of solvent/base: acetonitrile/DIEA, chloroform/DIEA and methanol/DIEA (Table 1, entries 5–9). In the presence of solvent/base: acetonitrile/DIEA, the highest yield of the intermediate **15** was obtained (85%, Table 1 entry 7).

The next step included transaminolysis of the intermediate **15** with cyclopropylamine **17** in the presence of 1,8-diazabicyclo [5.4.0]undec-7-ene (DBU) as an efficient catalyst to afford quinolone derivative **18**. We started to test of the cyclization reaction under batch and microwave conditions using DBU (20 mol %) in DMSO, the corresponding product **18** was obtained 20 and 52% in yield (Table 2, entries 2 and 5). Promoted by these results, the effect of DBU concentration was tested to find optimal conditions by changing mol % of DBU as illustrated in Table 2. Increasing the catalyst loading to 40 mol% gave the highest yield of the quinolone derivative **18** (80%, Table 2 entry 7). By increasing the amount of catalyst from 40 to 50 mol %, no a significant yield of the corresponding product **18** was collected (Table 2, entry 8). When the reaction time was increased to 30 min in the presence of DBU (40 mol %), there was a drop in the yield to 34% (Table 2, entry 9). From the optimal conditions, 40 mol % DBU and 25 min were chosen to be the best conditions to achieve the condensation of the intermediate **15** with cyclopropylamine **17** in a quantitative yield. Thus, we applied the microwave conditions which are listed in (Table 2, entry 7) as a conventional method for the synthesis of quinolone derivative **19** using the intermediate **16** instead of the intermediate **15**. The corresponding quinolone derivative **19** was subsequently collected 76% in yield.

Table 2 The optimal conditions for the synthesis of quinolone derivative **18**

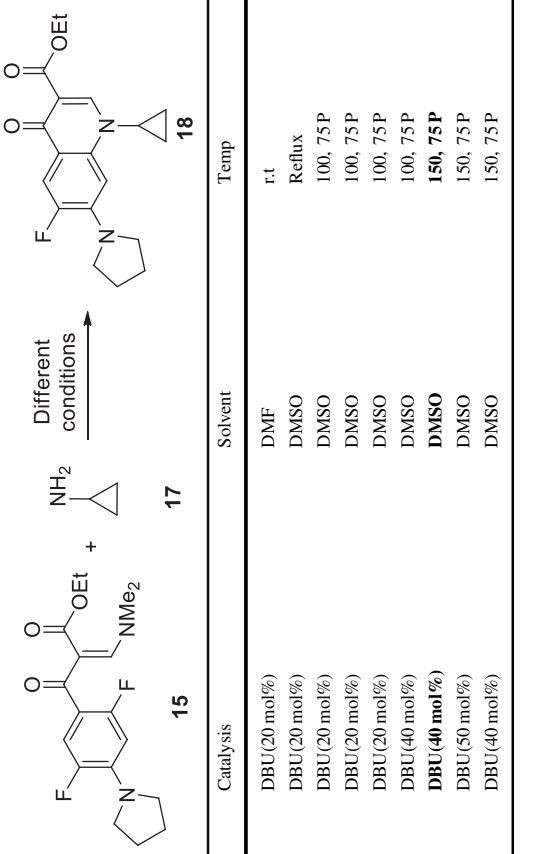

Entry	Method	Catalysis	Solvent	Temp	Time	Yield %[a]
1	Batch	DBU(20 mol%)	DMF	r.t	24 h	0
2	Batch	DBU(20 mol%)	DMSO	Reflux	4 h	20
3	MW	DBU(20 mol%)	DMSO	100, 75 P	5 min	–
4	MW	DBU(20 mol%)	DMSO	100, 75 P	10 min	–
5	MW	DBU(20 mol%)	DMSO	100, 75 P	20 min	52
6	MW	DBU(40 mol%)	DMSO	100, 75 P	20 min	63
7	**MW**	**DBU(40 mol%)**	**DMSO**	**150, 75 P**	**25 min**	**80**
8	MW	DBU(50 mol%)	DMSO	150, 75 P	25 min	50
9	MW	DBU(40 mol%)	DMSO	150, 75 P	30 min	34

[a]Isolated as a pure product

The purification of the synthesized quinolone derivatives **18** and **19** was performed with purity >96% as determined by their NMR, HPLC analysis and mass spectrometry (see supporting information). The ^{1}H, ^{9}F, ^{13}C NMR, FTIR and mass spectra data of all synthetic quinolone derivatives are consistent with the expected structures. The ^{1}H NMR spectra of quinolone derivatives **18** and **19** show one single at 8.10–8.30 ppm for fused quinolone proton (C=CH groups) at the expected region. In the ^{13}C NMR spectrum of all synthesized quinolone derivatives, the appearance of two signals at the lowest field is due to the carbon resonance of C=O and C=S groups. The other chemical shifts of ^{13}C NMR spectra are shown in the expected regions.

The geometries of quinolone derivatives **18** and **19** have been optimized by using density functional theory (DFT/B3LYP) calculations with the 6-311G (d, p) basis set. The optimized structures of quinolone derivatives **18** and **19** are shown in Fig. 2.

Protein–ligand docking is a powerful tool to investigate and provide a proper understanding for protein–ligand interactions in order to facilitate the design of potentially active lead compounds (Elokely and Doerksen 2013; Huang and Zou 2010; Sousa et al. 2006). The calculated binding energies for compounds **18** and **19** are −8.7 and −8.8 kcal mol^{-1} which indicate the compounds **18** and **19**

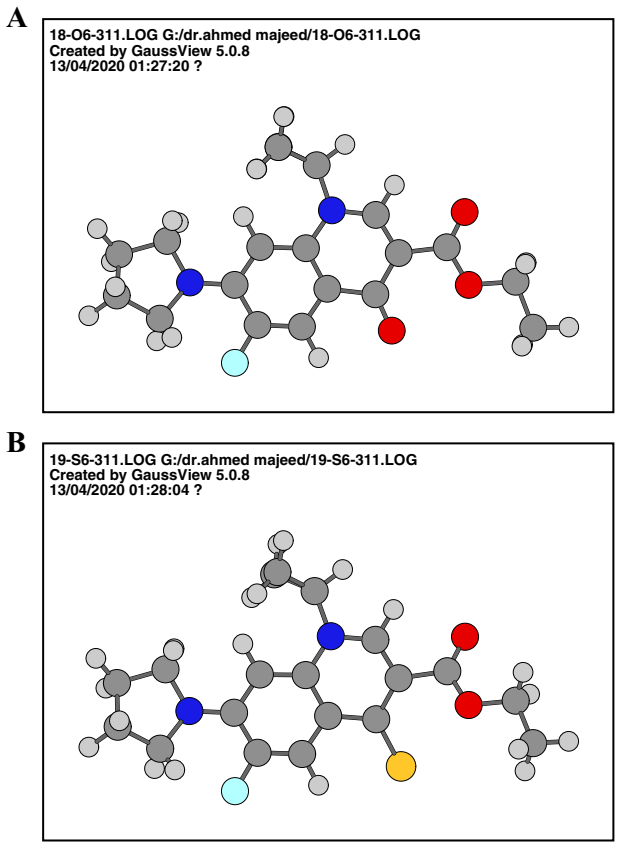

Fig. 2 Optimized structures of quinolone derivatives **18** and **19**

Table 3 Calculated binding energies and H-bond count of the targeted compounds **18** and **19** inside the human HER2 (PDB ID: 3PP0) active site

Comp	Binding energy (kcal/mol)	Protein–ligand interaction			
		H-bond count	Amino acid residues	Distance (Å)	Other interacting residues
18	−8.8	1	Lys753	3.32	Asp863, Thr798, Thr862, Ala751, Leu852, Leu800, Met801, Phe1004, Leu726, Cys804, Val734
19	−8.7	1	Lys753	3.18	Asp863, Thr798, Thr862, Ala751, Leu852, Leu800, Met801, Phe1004, Leu726, Cys804, Val734, Leu796

show a good selectivity for binding to an active site of the protein HER2 ATP-binding pocket as shown in Table 3. The molecular docking results also revealed that the synthesized compounds **18** and **19** could interact with Lys753 residues in the HER2 ATP-binding pocket. These compounds **18** and **19** were well fitted into the binding site of human HER2 by hydrogen bonds and other close interactions. The interactions of the HER2 protein with compounds **18** and **19** are shown in the Fig. 3. The docking of each compound showed the presence of one hydrogen bond interaction in the docked pose with amino acid residue (Lys753) as well as with hydrogen bond distances of 3.32 Å for compound **18** and 3.18 Å for compound **19**. The hydrogen bonding between the compounds (**18** and **19**) and receptor HER2 are shown in ball-and-stick representation. A few non-bonded interactions (Van der Waals interactions) are found between the compounds **18** and **19** and the residues Asp863, Thr798, Thr862, Ala751, Leu852, Leu800, Met801, Phe1004, Leu726, Cys804, and Val734. The residues that interact with compounds **18** and **19** via Van der Waals interactions are drawn as labeled arcs with radial spokes (Fig. 3).

PyMOL (DeLano) is a powerful source program for a molecular visualization which allows to extend the capabilities of the program *via* plugins (Gaudreault et al. 2015). The PyMOL molecular graphics system (version 2.0 Schrödinger, LLC) is used to generate qualitative pictures of molecular structures of the compounds **18** and **19**. The PyMOL offers multiple advanced rendering options and exceptional 3D viewing functionalities which are very useful in structure-based drug design (Fig. 4).

PyMOL plugin permits the detection of the surface cavities in proteins (Yuan et al. 2017). The protein (HER2) surface is shown as a cartoon (Fig. 5), showing the size of binding pocket and the electrostatic properties.

Quinolone derivatives **18** and **19** were screened for their in vitro anti-HIV-1 (strain III_B) and HIV-2 (strain ROD) activities in human T-lymphocyte (MT-4) cells based on an MTT assay. The results are summarized in Table 4. The data of nevirapine (BOE/BIRG587) and azidothymidine (DDN/AZT) are included for comparison.

Quinolone derivatives-induced cytotoxicity were also measured in MT-4 cells parallel with antiviral activity. All these derivatives are active which showed IC_{50} values of ≥15.20 μM ($CC_{50} = 89.68$ μM) and 14.26 μM ($CC_{50} =>$ 105.00 μM) against HIV-1 (strain III_B), resulting selectivity index (SI) values of ≤6, >7, respectively.

With respect to structure-activity relationship studies, quinolone derivatives trigger significant activities as HIV-1 inhibitors. As regards with the electronic nature of the substituents of the synthesized compounds, both pyrrolidine and quinolone groups showed good activities. Accordingly, the combined four portions (pyrrolidine, quinolone, pyridin-4(1H)-one residue, and carboxylate moiety) of quinolone derivatives **18** and **19** are considered as the optimal substituents that would offer an enhancement to the optimal activity.

Our results showed that the quinolone derivatives **18** and **19** were found to be potent agents against HIV-1 (strain III_B). Thus, these compounds might be considered as promising agents for further pharmacological evaluation.

Conclusion

We have improved that microwave methodology can be successfully used to synthesize of potential bioactive quinolone derivatives. This method is an innovative tool for improvement of cyclization reactions without any difficulties to achieve a nucleophilic ring closure system. Molecular docking studies have been used to investigate any interaction that exists between the synthesized compounds and the residues lies in the active site cavity of human epidermal growth factor receptor 2 HER2 (PDB ID: 3PP0). Docking study also showed hydrogen bonding, polar and van der Waals interactions with the active site residues of HER2 target. In addition, the new synthesized quinolone derivatives were evaluated against HIV-1 (strain III_B) and HIV-2 (strain ROD), and the results showed these derivatives have a potent activity against HIV-1 replication. Our results may help to design new quinolone derivatives with a high pharmacological importance in the future. Further studies in an in vitro for evaluating anti-breast cancer activity of these derivatives are in progress.

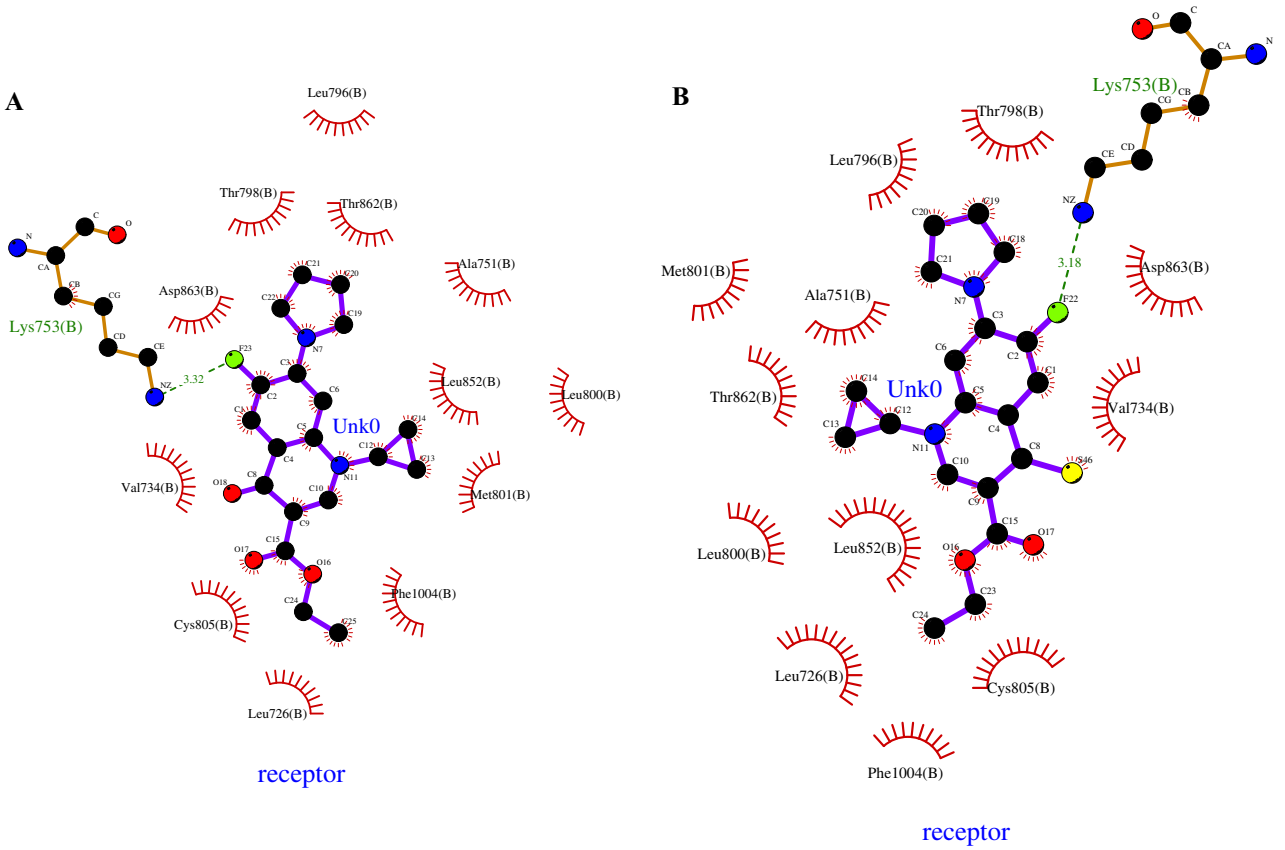

Fig. 3 2D interactions of compounds **18** (**a**) and **19** (**b**) with the HER2

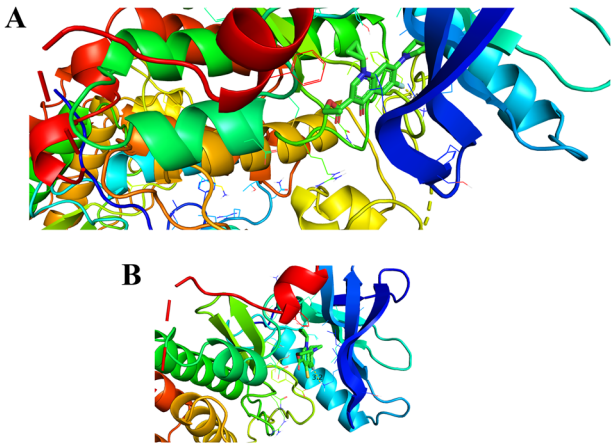

Fig. 4 3D ligand-receptor interactions between compounds **18** (**a**) and **19** (**b**), interactions with the progesterone receptor HER2 using PyMOL Version 2.0 Schrödinger, LLC

Acknowledgements Funding for this work was performed by the authors. We gratefully thank to Leicester University, UK for ^{1}H, ^{13}C NMR, FTIR, HRMS spectra and HPLC. We also thank the staff (Cell and Molecular Biology Lab, Department of Zoology and Cytology, Government College University, Faisalabad, Pakistan for the anti-HIV screening.

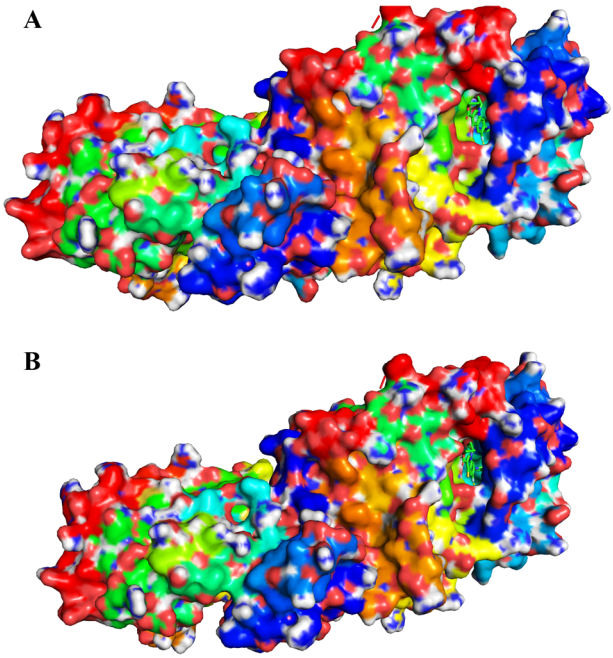

Fig. 5 Representations of compounds **18** (**a**) and **19** (**b**) and the surface carton protein (PDB: 3PP0) stereo mode in PyMOL

Table 4 In vitro anti-HIV-1 and HIV-2 activities of quinolone derivatives **18** and **19**

Comp	V. strain (III_B[a] and ROD[b])	av.IC_{50} (μM)[c]	av.CC_{50} (μM)[d]	SI[e]
(**18**)	III_B	≥15.20	89.68	≤6
	ROD	>89.69	89.69	X1
(**19**)	III_B	14.26	>105.00	>7
	III_B	>115.00	>115.00	X1
Nevirapine	III_B	0.05	>4.00	>80
	ROD	>4.00	>4.00	<1
AZT	III_B	0.0019	>25	>13144
	ROD	0.0018	>25	>14245

All data represent the mean values that were obtained from three separate experiments

[a]Anti-HIV-1 activity measured against strain III_B

[b]Anti-HIV-2 activity measured against strain ROD

[c]Compound concentration required to achieve 50% protection of MT-4 cells from the HIV-1 and 2-induced cytopathogenic effect

[d]Average CC50: compound concentration that reduces the viability of the mock-infected MT-4 cells by 50%

[e]SI: selectivity index (CC50/IC50)

Compliance with ethical standards

Conflict of interest The authors declare that they have no conflict of interest.

Ethical approval This article does not contain any studies with human participants or animals performed by any of the authors.

Publisher's note Springer Nature remains neutral with regard to jurisdictional claims in published maps and institutional affiliations.

References

Amore KM, Leadbeater NE, Miller TA, Schmink JR (2006) Fast, easy, solvent-free, microwave-promoted Michael addition of anilines to α,β-unsaturated alkenes: synthesis of *N*-aryl functionalized β-amino esters and acids. Tetrahedron Lett 47:8583–8586

Anquetin G, Greiner J, Vierling P (2005) Quinolone-based drugs against toxoplasma gondii and plasmodium spp. Curr Drug Targets-Infec Diso 5:227–245

Appelbaum PC, Hunter PA (2000) The fluoroquinolone antibacterials: past, present and future perspectives. Int J Antim Agen 16:5–15

Baker WR, Cai S, Dimitroff M, Fang L, Huh KK, Ryckman DR, Shang X, Shawar RM, Therrien JH (2004) A prodrug approach toward the development of water soluble fluoroquinolones and structure−activity relationships of quinoline-3-carboxylic acids. J Med Chem 47:4693–4709

Beberok A, Wrześniok D, Rzepka Z, Rok J, Delijewski M, Otręba M, Respondek M, Buszman E (2017) Effect of fluoroquinolones on melanogenesis in normal human melanocytes HEMn-DP: a comparative in vitro study. Cutan Ocul Toxicol 36:169–175

Bisacchi GS (2015) Origins of the quinolone class of antibacterials: an expanded "discovery story". J Med Chem 58:4874–4882

Chavain N, Vezin H, Dive D, Touati N, Paul JF, Buisine E, Biot C (2008) Investigation of the redox behavior of ferroquine, a new antimalarial. Mol Pharm 5:710–716

Chevalier J, Atifi S, Eyraud A, Mahamoud A, Barbe J, Pagès JM (2001) New pyridoquinoline derivatives as potential inhibitors of the fluoroquinolone efflux pump in resistant enterobacter aerogenes strains. J Med Chem 44:4023–4026

Dahl EL, Rosenthal PJ (2007) Multiple antibiotics exert delayed effects against the *plasmodium falciparum* apicoplast. Antimicrob Agents Chemother 51:3485

Dalhoff A (2015) Antiviral, antifungal, and antiparasitic activities of fluoroquinolones optimized for treatment of bacterial infections: a puzzling paradox or a logical consequence of their mode of action. Eur J Clin Microbio Infec Dis 34:661–668

Dent S, Oyan B, Honig A, Mano M, Howell S (2013) HER2-targeted therapy in breast cancer: a systematic review of neoadjuvant trials. Cancer treat rev 39:622–631

Driowya M, Saber A, Marzag H, Demange L, Bougrin K, Benhida R (2016) Microwave-assisted syntheses of bioactive seven-membered, macro-sized heterocycles and their fused derivatives. Molecules 21:1032

Drlica K, Hiasa H, Kerns R, Malik M, Mustaev A, Zhao X (2009) Quinolones: action and resistance updated. Curr Top Med Chem 9:981–998

Drlica K, Malik M (2003) Fluoroquinolones: action and resistance. Curr Top Med Chem 3:249–282

Dubar F, Khalife J, Brocard J, Dive D, Biot C (2008) Ferroquine, an ingenious antimalarial drug –thoughts on the mechanism of action. Molecules 13:2900–2907

Dubar F, Wintjens R, Martins-Duarte ÉS, Vommaro RC, de Souza W, Dive D, Pierrot C, Pradines B, Wohlkonig A, Khalife J (2011) Ester prodrugs of ciprofloxacin as DNA-gyrase inhibitors: synthesis, antiparasitic evaluation and docking studies. Med Chem Comm 2:430–435

Elokely KM, Doerksen RJ (2013) Docking challenge: protein sampling and molecular docking performance. J Chem Inf Mode 53:1934–1945

Gaudreault F, Morency LP, Najmanovich RJ (2015) NRGsuite: a PyMOL plugin to perform docking simulations in real time using FlexAID. Bioinformatics 31:3856–3858

Hajimahdi Z, Zabihollahi R, Aghasadeghi MR, Ashtiani SH, Zarghi A (2016) Novel quinolone-3-carboxylic acid derivatives as anti-HIV-1 agents: design, synthesis, and biological activities. Med Chem Res 25:1861–1876

Huang SY, Zou X (2010) Advances and challenges in protein-ligand docking. Int J Mol Sci 11:3016–3034

Jacoby GA (2005) Mechanisms of resistance to quinolones. Clin Infec Dis 41:120–126

Jardosh HH, Patel MP (2013) Microwave-assisted CAN-catalyzed solvent-free synthesis of N-allyl quinolone-based pyrano[4,3-b] chromene and benzopyrano[3,2-c]chromene derivatives and their antimicrobial activity. Med Chem Res 22:905–915

Jida M, Deprez-Poulain R, Malaquin S, Roussel P, Agbossou-Niedercorn F, Deprez B, Laconde G (2010) Solvent-free microwave-assisted Meyers' lactamization. Green Chem 12:961–964

Kappe CO, Dallinger D (2009) Controlled microwave heating in modern organic synthesis: highlights from the 2004–2008 literature. Mol Div 13:71

Kumar S, Patel A, Ahmed N (2015) Microwave-assisted expeditious and efficient synthesis of novel quinolin-4-ylmethoxychromen-2- and -4-ones catalyzed by YbCl3 under a solvent free one-pot three component domino reaction and their antimicrobial activity. RSC Adv 5:93067–93080

Kumar S, Verma N, Ahmed N (2018) Microwave assisted highly efficient one-pot multi-component synthesis of novel 2-(tetra-substituted-1H-pyrrol-3-yl)-4H-chroman-4-ones catalyzed by heterogeneous reusable silica gel supported polyphosphoric acid (PPA/SiO2). J Saudi Chem Soc 22:136–145

Laponogov I, Sohi MK, Veselkov DA, Pan XS, Sawhney R, Thompson AW, McAuley KE, Fisher LM, Sanderson MR (2009) Structural

insight into the quinolone–DNA cleavage complex of type IIA topoisomerases. Nat Str Amp; Mol Bio 16:667

Lee C, Yang W, Parr RG (1988) Development of the colle-salvetti correlation-energy formula into a functional of the electron density. Phy rev B 37:785

Maiti B, Chanda K (2016) Diversity oriented synthesis of benzimidazole-based biheterocyclic molecules by combinatorial approach: a critical review. RSC Adv 6:50384–50413

Matrat S, Cambau E, Jarlier V, Aubry A (2008) Are all the DNA qyrase mutations found in *mycobacterium leprae* clinical strains involved in resistance to fluoroquinolones? Antimicrob Agents Chemother 52:745

Matrat S, Petrella S, Cambau E, Sougakoff W, Jarlier V, Aubry A (2007) Expression and purification of an active form of the *mycobacterium leprae* DNA Gyrase and its inhibition by quinolones. Antimicrob Agents Chemother 51:1643

Mitscher LA (2005) Bacterial topoisomerase inhibitors: quinolone and pyridone antibacterial agents. Chem Rev 105:559–592

Naqvi SAR, Roohi S, Iqbal A, Sherazi TA, Zahoor AF, Imran M (2018) Ciprofloxacin: from infection therapy to molecular imaging. Mole Bio Rep. 45:1457–1468

Patpi SR, Pulipati L, Yogeeswari P, Sriram D, Jain N, Sridhar B, Murthy R, T AD, Kalivendi SV, Kantevari S (2012) Design, synthesis, and structure–activity correlations of novel dibenzo[b,d]furan, dibenzo[b,d]thiophene, and *N*-methylcarbazole clubbed 1,2,3-triazoles as potent inhibitors of mycobacterium tuberculosis. J Med Chem 55:3911–3922

Pauwels R, Balzarini J, Baba M, Snoeck R, Schols D, Herdewijn P, Desmyter J, De Clercq E (1988) Rapid and automated tetrazolium-based colorimetric assay for the detection of anti-HIV compounds. J Virolo meth 20:309–321

Payne DJ, Gwynn MN, Holmes DJ, Pompliano DL (2006) Drugs for bad bugs: confronting the challenges of antibacterial discovery. Nat Rev Drug Dis 6:29

Pinhel I, Hills M, Drury S, Salter J, Sumo G, A'Hern R, Bliss JM, Sestak I, Cuzick J, Barrett-Lee P (2012) ER and HER2 expression are positively correlated in HER2 non-overexpressing breast cancer. Breast Cancer Res 14:46

Seijas JA, Vázquez-Tato MP, Crecente-Campo J (2008) Straightforward microwave-assisted synthesis of 2-thiazolines using Lawesson's reagent under solvent-free conditions. Tetrahedron 64:9280–9285

Shaabani A, Bazgir A (2004) Microwave-assisted efficient synthesis of spiro-fused heterocycles under solvent-free conditions. Tetrahedron Lett 45:2575–2577

Shanmugavelan P, Nagarajan S, Sathishkumar M, Ponnuswamy A, Yogeeswari P, Sriram D (2011) Efficient synthesis and in vitro antitubercular activity of 1,2,3-triazoles as inhibitors of Mycobacterium tuberculosis. Bioor Med Chem Lett 21:7273–7276

Siegel R, Ward E, Brawley O, Jemal A (2011) Cancer statistics, 2011. CA: A Cancer J Clin 61:212–236

Sousa SF, Fernandes PA, Ramos MJ (2006) Protein–ligand docking: current status and future challenges. Proteins: Str Fun Bioinfo 65:15–26

Spellberg B, Bartlett J, Wunderink R, Gilbert DN (2015) Novel approaches are needed to develop tomorrow's antibacterial therapies. Am J Resp Cri Care Med 191:135–140

Sravanthi S, Harinadha Babu V, Shiva R (2019) Design, synthesis, molecular docking, ADMET studies, and biological evaluation of isoxazoline and pyrazoline incorporating 1,2,3-triazole benzene sulfonamides. Russ J Bioorg Chem 45:381–390

Stockler M, Wilcken N, Ghersi D, Simes RJ (2000) Systematic reviews of chemotherapy and endocrine therapy in metastatic breast cancer. Cancer Treat Rev 26:151–168

Sumangala V, Poojary B, Chidananda N, Fernandes J, Kumari NS (2010) Synthesis and antimicrobial activity of 1,2,3-triazoles containing quinoline moiety. Arch Pharm Res 33:1911–1918

Trott O, Olson AJ (2010) AutoDock Vina: improving the speed and accuracy of docking with a new scoring function, efficient optimization, and multithreading. J Comput Chem 31:455–461

Vracar TC, Zuo J, Park J, Azer D, Mikhael C, Holliday SA, Holsey D, Han G, VonMoss L, Neubert JK, Rody WJ, Chan EL, Holliday LS (2018) Enoxacin and bis-enoxacin stimulate 4T1 murine breast cancer cells to release extracellular vesicles that inhibit osteoclastogenesis. Sci Rep. 8:16182

Wohlkonig A, Chan PF, Fosberry AP, Homes P, Huang J, Kranz M, Leydon VR, Miles TJ, Pearson ND, Perera RL, Shillings AJ, Gwynn MN, Bax BD (2010) Structural basis of quinolone inhibition of type IIA topoisomerases and target-mediated resistance. Nat Str Amp Mol Biol 17:1152

Yuan S, Chan HS, Hu Z (2017) Using PyMOL as a platform for computational drug design. Comp Mol Sci 7:1298

Zelmat Y, Rousseau V, Chebane L, Montastruc JL, Bagheri H, Sommet A (2020) Fluoroquinolone-induced photosensitivity: a chemical fragment-based approach by a case/non-case study in vigibaser®. Drug Safety 43:535